[94] These authors also propose that an absorption in germanium at 11.6 microns is due to similar Ge-O vibrations.
[95] Hrostowski, H. J., and Kaiser, R. H. "Infrared Absorption of Oxygen in Silicon," *Physical Review*, Vol. 107 (August 15, 1957), pp. 966–972.
[96] Kaiser, W. "Properties of Heat-Treated Silicon," *Physical Review*, Vol. 105 (March 15, 1957), pp. 1751–1756.
[97] Lederhandler, S., and Patel, J. R. "Behavior of Oxygen in Plastically Deformed Silicon," *Physical Review*, Vol. 108 (October 15, 1957), pp. 239–242.
[98] Fuller and Logan [91] make the point that the difference in oxygen content does not seem large enough, however, to explain the difference in the number of donors produced in heat treatment.
[99] Kaiser, W., and Keck, P. H. "Oxygen Content of Silicon Single Crystals," *Journal of Applied Physics*, Vol. 28 (August, 1957), pp. 882–887.
[100] Dash, W. C. "Birefringence in Silicon," *Physical Review*, Vol. 98 (June 1, 1955), p. 1536.
[101] Hannay, N. B., Haynes, J. R., and Shulman, R. G. "The Interaction of Traps and Heat Treatments in Silicon," *Physical Review*, Vol. 96 (November 1, 1954), p. 833.
[102] Pearson, G. L., Read, W. T., and Feldmann, W. L. "Deformation and Fracture of Small Silicon Crystals," *Bulletin of the American Physical Society*, Ser. II, Vol. 1 (June, 1956), p. 295.
[103] Logan, R. A., and Peters, A. J. "Effect of Oxygen on Etch-Pit Formation in Silicon," *Journal of Applied Physics*, Vol. 28 (December, 1957), pp. 1419–1423.
[104] Bemski, G., and Struthers, J. D. "Gold in Silicon," *Journal of the Electrochemical Society*, to be published. The author is indebted to Dr. Bemski for making the manuscript available prior to publication.
[105] Fan, H. Y., Shepard, M. L., and Spitzer, W. "Infrared Absorption and Energy-Band Structure of Germanium and Silicon" in *Photoconductivity Conference*.
[106] Dash, W. C., and Newman, R., "Intrinsic Optical Absorption in Single Crystal Germanium and Silicon at 77°K and 300°K," *Physical Review*, Vol. 99, August 15, 1955, pp. 1151–1155.
[107] Avery, D. G., and Clegg, P. L. "Optical Constants of Single Crystals of Germanium," *Proceedings of the Royal Society B, London*, Vol. 66 (June, 1953), pp. 512–513.
[108] Pfestorf, G. "Optical Constant of Metals in the Visible and Ultraviolet Region of the Spectrum," *Annalen der Physik*, Vol. 81 (December, 1926), pp. 906–928.
[109] Tyler, W. W. "Properties of Ag-Doped Germanium," *Bulletin of the American Physical Society*, Ser. II, Vol. 3 (March, 1958), p. 128.
[110] Dunlap, W. C., Jr. "Properties of Zn-, Cu- and Pt-Doped Germanium," *Physical Review*, Vol. 96 (October 1, 1954), pp. 40–45.
[111] Woodbury, H. H., and Tyler, W. W. "Properties of Zn-Doped Germanium," *Physical Review*, Vol. 100 (November 15, 1955), p. 1259.
[112] ——. "Recent Studies of Deep Impurity Levels in Ge," *Bulletin of the American Physical Society*, Ser. II, Vol. 1 (March, 1956), p. 127.
[113] Geballe, T. H., and Morin, F. J. "Ionization Energy of Groups III and V Elements in Germanium," *Physical Review*, Vol. 95 (August 16, 1954), pp. 1085–1086.
[114] Woodbury, H. H., and Tyler, W. W. "Properties of Germanium Doped with Manganese," *Physical Review*, Vol. 100 (October 15, 1955), pp. 659–662.
[115] Morin, F. J., Maita, J. P., Shulman, R. G., and Hannay, N. B. "Impurity Levels in Silicon," *Bulletin of the American Physical Society*, Vol. 29 (June, 1954), p. 22.
[116] Carlson, R. O. "Double-Acceptor Behavior of Zinc in Silicon," *Physical Review*, Vol. 108 (December 15, 1957), pp. 1390–1393.
[117] ——. "Properties of Silicon Doped with Manganese," *Physical Review*, Vol. 104 (November 15, 1956), pp. 937–941.

Correspondence

Parametric Amplification of the Fast Electron Wave*

The concept of space charge waves in electron streams is widely known. Restoring forces, generated in velocity modulation tubes by space charge fields and in transverse field tubes by the focusing field, produce a pair of such waves, commonly called the slow and the fast wave. Their phase velocities are

$$u_{12} = u_e \frac{\omega_1}{\omega_1 \pm \omega_e}$$

(u_e = velocity of stream; ω_1 = signal frequency; ω_e = resonant frequency corresponding to the restoring mechanism, such as plasma frequency or cyclotron frequency).

Conventional traveling-wave tubes employ interaction between a circuit and the slow electron wave to produce gain. It appears to be established[1] that the noise present in this wave cannot be removed.

On the other hand, noise cancellation is possible for the fast electron wave; interaction with this wave, unfortunately, does not produce gain in conventional devices.

It would be of great interest to construct a device which employs fast-wave interaction in its input and output sections and in which the amplitude of electron motion is increased between input and output by other means. Such an increase in amplitude might be obtained by utilizing an old principle which recently has become more widely known as parametric amplification. This method is based on nonlinear effects. It requires an external power source of large amplitude, operating at a pumping frequency ω_3 which must be higher than the signal frequency ω_1. An auxiliary resonant mesh must be provided at the beat frequency $\omega_2 = \omega_3 - \omega_1$, except in the special case where $\omega_3 = 2\omega_1$. A thorough discussion of this method was given by Manley and Rowe.[2]

As an example of a fast-wave device to which parametric amplification might be applied, consider Cuccia's electron coupler[3] (Fig. 1). This is a transverse field device, consisting of two lumped resonant cavities through which an electron stream flows; a homogeneous magnetic field confines this stream, its intensity so chosen that the cyclotron frequency equals the signal frequency. A signal applied to the first cavity

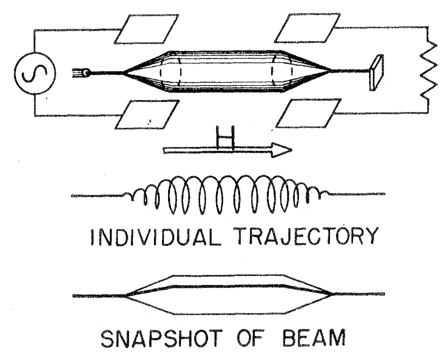

Fig. 1.

causes the electrons to spiral outward. They reach a maximum radius at the exit of the first cavity; at this point, all the signal power supplied appears in the form of kinetic energy.

In the second cavity the orbiting electrons induce a current and if the cavity is properly loaded, the resulting field causes them to spiral inward and give up all their energy.

There is no gain in this device and no interchange of energy occurs between the transverse signal motion and the longitudinal forward motion. All electrons throughout the device orbit in phase; the phase velocity is infinite in accordance with the condition $\omega_1 = \omega_e$.

* Received by the IRE, January 6, 1958. Presented at the Conference on Electron Tube Research, Berkeley, Calif., June, 1957.

[1] H. A. Haus and F. N. H. Robinson, "The minimum noise figure of microwave beam amplifiers," PROC. IRE, vol. 43, pp. 981–991; August, 1955.

[2] J. M. Manley and H. E. Rowe, "Some general properties of nonlinear elements," PROC. IRE, vol. 44, pp. 904–913; July, 1956.

[3] C. L. Cuccia, "The electron coupler," *RCA Rev.* vol. 10, pp. 270–303; June, 1949.

The second cavity absorbs from the stream all the available fast-wave signal power. The first cavity, properly loaded by a resistive source, should similarly absorb all the fast-wave noise power, leaving the stream quiet. This has been demonstrated (Fig. 2).

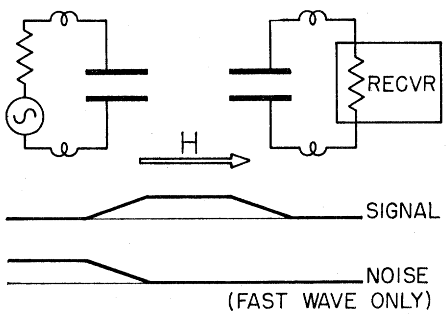

Fig. 2.

A small tube was built, using a strip beam of 200 μa at 6 volts in a magnetic field of about 180 Gauss. The two cavities were formed by two pairs of deflection plates, each pair having 1-cm length in the direction of beam travel, 1.5-cm width and 0.075-cm spacing. The two pairs were shielded from each other and tuned externally. Measurements were made at 528 mc.

A noise minimum was observed when the input circuit was carefully tuned and properly loaded and the magnetic field was correctly adjusted. Under these conditions signal transmission was also best.

Parametric amplification of the transverse electron motion could be produced by applying the pumping signal to an electrode system which produces an inhomogeneous transverse field across the stream. A fence-like array of electrodes of alternating polarity meets this purpose. Fig. 3 shows the pro-

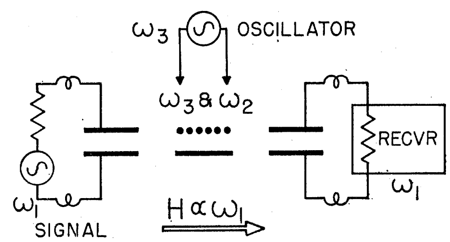

Fig.

posed arrangement. For greater clarity, the fence posts are shown positioned at right angles to the direction of beam travel; it might be better to arrange them parallel to that direction.

As previously stated, the array must be tuned to the beat frequency ω_2, unless the pumping frequency ω_3 is very nearly equal to twice the signal frequency ω_1.

An arrangement of this kind, employing parametric amplification between two fast-wave beam coupling devices, may well result in a very low noise figure.

Robert Adler
Zenith Radio Corp.
Chicago, Ill.

Experimental Characteristics of a Microwave Parametric Amplifier Using a Semiconductor Diode*

The purpose of this letter is to report our observation of the characteristics of a microwave parametric amplifier[1-3] which we have constructed recently. The amplifier employs a back-biased germanium junction diode placed between central posts inside a rectangular cavity as shown in Fig. 1. With proper adjustments of the tuning screws, the cavity with diode in place can be made simultaneously resonant at 3500 mc, 2300 mc, and 1200 mc. We believe these three resonances are the perturbed TE_{103}, TE_{301}, and TE_{101} modes of the empty rectangular box. A loop serves to couple into the 3500-mc resonance and two probes serve to couple in and out of the cavity at either the 1200-mc or the 2300-mc resonance. With proper adjustment they can be made to couple predominantly to the 1200-mc resonance with an insertion loss which depends upon diode bias but is typically 4 to 6 db.

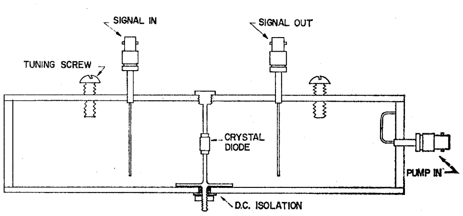

Fig. 1—Cross-section of variable-parameter amplifier.

The diode[4] which was kindly supplied through the Evans Signal Laboratory has a low-frequency zero-bias capacitance of 1 $\mu\mu$f and a spreading resistance of 5 ohms as measured on a standard impedance bridge.

With a pump power at 3500 mc applied to the cavity slightly in excess of 100 mw, the device oscillates at both 1200 mc and 2300 mc either with or without dc diode bias. Below this value of pump power, amplification can be obtained at either of the two frequencies. The majority of our measurements have so far been made on the operation of the device as an amplifier at the lowest of these frequencies using of the order of 5 volts diode bias.

We have been able to obtain net gain up to 40 db, although at such high gains the amplifier is extremely sensitive to load variations since no isolator or circulator is employed. Moreover, there is some noticeable gain variation due to the residual frequency modulation of the 3500-mc pump generator (a Hewlett-Packard signal generator followed by a 1 watt TW tube and filter). The bandwidth at 19 db gain is 1.0 mc and follows the predicted relation-gain times bandwidth squared equals a constant. The saturated power output is approximately 1.5 mw. The dynamic range is over 100 db.

Our preliminary measurement of noise figure at 16 db gain indicates the noise figure is less than 4.8 db.

H. Heffner
K. Kotzebue
Electronics Labs.
Stanford University
Stanford, Calif.

* Received by the IRE, March 24, 1958. This work was performed under a supported joint Services research contract N6ONR 225(24) while K. Kotzebue held a Bell Telephone Laboratories Fellowship.

[1] H. Suhl, "Proposal for a ferromagnetic amplifier in the microwave range," *Phys. Rev.*, vol. 106, pp. 384–385; April 15, 1957.

[2] M. E. Hines proposed the use of a semiconductor diode as a variable element and reported some experimental results at the Annual Conference on Electron Tube Research, Berkeley, Calif.; June, 1957.

[3] H. Heffner and G. Wade reported an analysis of of the noise figure and gain-bandwidth characteristics of the parametric amplifier at the Annual Conference on Electron Tube Research.

[4] This type of diode was developed by A. Uhlir, Bell Telephone Laboratories, and has been given the number W.E.427A.

Noise Figure Measurements on Two Types of Variable Reactance Amplifiers Using Semiconductor Diodes*

The purpose of this letter is to report experimental results on low-noise amplification at uhf and microwave frequencies by *p-n* junction diodes. Some twelve years have passed since amplification by semiconductor diodes was first reported[1] in an experiment involving frequency conversion from 10,000 mc to 30 mc. The noise figures obtained were not encouraging, and the work was discontinued. Recent studies [2-4] show that up-conversion from a low frequency to a high frequency is more likely to produce stable, low-noise amplification.

Low-noise performance also has been predicted for microwave amplification involving a negative resistance type of diode interaction[5] and experimental verification of the gain mechanism of such an amplifier has been achieved.[6]

Measurements which bear out the theoretically predicted low-noise performance of both the negative resistance amplifier and the up-converter are described. The lowest noise figures reported here have been obtained using special diffused silicon *p-n* junction diodes[7] having small capacitance and very low values of series resistance. Further information on the properties and prospec-

* Received by the IRE, April 4, 1958. This work was supported in part by the U. S. Army Signal Corps.

[1] H. C. Torrey and C. A. Whitmer, "Crystal Rectifiers," M.I.T. Rad. Lab. Ser., McGraw-Hill Book Co., Inc., New York, N. Y., vol. 15, ch. 13; 1948.

[2] A. Uhlir, Jr., "Two-terminal *p-n* junction devices for frequency conversion and computation," Proc. IRE, vol. 44, pp. 1183–1191; September, 1956.

[3] "Semiconductor Diodes Yield Converter Gain," Bell Labs. Rec., vol. 35, p. 412; October, 1957.

[4] A. Uhlir, Jr., "Diffused Silicon and Germanium Nonlinear Capacitors," presented at the IRE-AIEE Semiconductor Device Research Conf., Boulder, Colo.; July, 1957.

[5] M. E. Hines, paper submitted for publication.

[6] M. E. Hines, "Amplification in Nonlinear Reactance Modulators," presented at the 15th Annual Conf. on Electron Tube Research, Berkeley, Calif.; June, 1957.

[7] A. E. Bakanowski, N. G. Cranna, and A. Uhlir, Jr., "Diffused Germanium and Silicon Nonlinear Capacitor Diodes," presented at the IRE-AIEE Semiconductor Device Research Conf., Boulder, Colo.

tive uses of these diodes will be found elsewhere.[8]

The fundamental power relations for a nonlinear (lossless) reactance are summed up by a theorem due to Manley and Rowe.[9] When a strong local oscillator or pump of frequency f_p and a signal of frequency f_s are impressed simultaneously on a nonlinear reactance, frequencies equal to mf_p+nf_s are produced. If one considers only the signal and the two lowest sidebands, f_{p-s} and f_{p+s}, and ignores all of the other higher order modulation products, then the power relation due to Manley and Rowe becomes

$$\frac{P_s}{f_s}+\frac{P_{p+s}}{f_{p+s}}-\frac{P_{p-s}}{f_{p-s}}=0 \qquad (1)$$

where P_s, P_{p+s}, and P_{p-s} are the powers at frequencies f_s, f_{p+s}, and f_{p-s}. A positive value of P denotes power generated by the amplifier, and a negative value denotes power absorbed by the amplifier.

In the simplest version of the up-converter, the circuit is tuned to f_s and f_{p+s} only, and (1) becomes

$$P_{p+s}+\frac{f_{p+s}}{f_s}P_s=0. \qquad (2)$$

Under these conditions P_s and P_{p+s} have opposite signs so that power will be emitted at f_{p+s} when signal power is being supplied at f_s; furthermore, the emitted power will exceed the signal power, the power ratio or gain being equal to f_{p+s}/f_s. The relation also shows that gain at the signal frequency is impossible because the difference in signs for P_s and P_{p+s} would require that a positive value of P_s be accompanied by an even larger expenditure of signal power at f_{p+s}.

In the simple negative resistance amplifier, on the other hand, the circuit is tuned only to f_s and its "image" f_{p-s} so that (1) becomes

$$\frac{P_s}{f_s}=\frac{P_{p-s}}{f_{p-s}}. \qquad (3)$$

Here P_s and P_{p-s} have like signs so that amplification at the signal frequency does not require absorption of signal power at another frequency. One therefore can have power gain in the ordinary sense that input power at f_s gives rise to an amplified power output at the same frequency. In this process, power will necessarily also be emitted at f_{p-s}. The amount of gain obtainable is limited only by the properties of the circuit and obeys a constant gain-bandwidth product relation. Gain under these conditions may be thought of as a negative resistance effect.

One also can allow all three signals to be present. In this case, gain can be obtained as a result of a frequency shift as well as from negative resistance effects. The general properties of such an amplifier are analyzed in detail in a forthcoming paper.[5]

[8] A. Uhlir, Jr., "The potential of semiconductor diodes in high-frequency communications," this issue, p. 1099.

[9] J. M. Manley and H. E. Rowe, "Some general properties of nonlinear elements—Part I. General energy relations," PROC. IRE, vol. 44, pp. 904–913; July, 1956.

The experimental results previously reported by Hines[6] were obtained using a point contact germanium diode with pump at 12,350 mc, and amplification was obtained at frequencies near 6175 mc. Under certain conditions of circuit adjustment, oscillations at precisely 6175 mc were also observed. These results are in accordance with the predictions of (3). Experimental results are given on the two types of parametric amplifier discussed above.

Up-Converter

An "up-converter" circuit was assembled in which the signal is introduced at 460 mc and the beating oscillator or "pump" at 8915 mc. The arrangement is shown schematically in Fig. 1. The output at the upper sideband, 9375 mc, was detected by a superheterodyne receiver using balanced point-contact crystals in conventional fashion to give a second-stage noise figure of 7 db. In typical operation, the up-converter gain was 9 db and the over-all noise figure, including noise from the second stage, was 2.5 ± 0.5 db. The first-stage (up-converter) noise figure was therefore 2 ± 0.5 db, which may also be expressed as a "noise temperature" of 170 $\pm50°$K. These measurements were obtained by standard noise lamp procedures. The over-all noise figure was checked, within the indicated accuracy, by using a refrigerated input load, and also with a signal generator of ±2-db accuracy. About 200 mw of pump power was absorbed, but 2 w of incident power was used to avoid having to provide a good match at the pump frequency. Reasonably broad-band amplification is predicted by the theory, but has not yet been achieved experimentally.

A particular adjustment of the circuit (which has not been reproducible at will) gave 21 db of gain and an over-all noise figure of 1.1 ± 0.5 db ($87\pm40°$K). Since the gain in this case exceeded the frequency ratio, 9375/460, this situation must have involved the lower sideband to a considerable extent.

Negative Resistance Amplifier

A negative resistance amplifier was designed to operate near 6 kmc with pump power at 11.7 kmc. The experimental setup is seen in Fig. 2. Amplification is obtained by returning more signal power into the input waveguide of the diode than was incident there, and a circulator is used to provide isolation between ingoing and outcoming waves. The circulator also prevents thermal noise originating in the load from being amplified.

The gain of the amplifier depends on pumping power level as well as on circuit adjustment. The pump requirement is simply one of obtaining a suitable voltage swing across the nonlinear capacitance. Hence a diode with a high value of C_0 (where C_0 is the static capacitance of the diode) will require in general more pump power than one with a low value, and a circuit which is high Q for the pump will be more efficient than a low-Q circuit. The amount of pump power used to obtain the results given below was between 50 and 500 mw with no special attempt made to optimize the pump circuit.

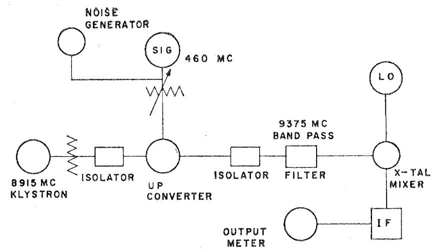

Fig. 1—Up-converter arrangement.

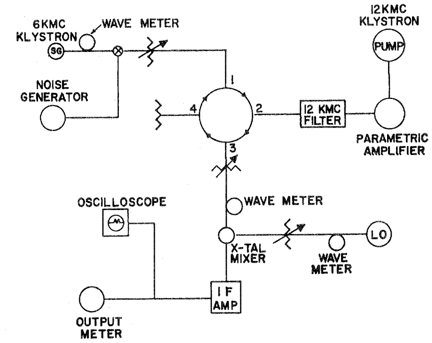

Fig. 2—Negative resistance amplifier arrangement.

Silicon and germanium diffused p-n junction diodes and welded-contact (gold-bonded) germanium diodes were used. Values of C_0 with no dc bias ranged from 0.4 to 2.85 mmf. The silicon junction diodes were usually operated with zero dc bias, but a negative bias voltage of from 1 to 1.5 volts was applied to the germanium diodes to reduce C_0 to a suitable value for optimum amplification. Stable power gains as high as 45 db were measured at $f_s=f_{p/2}$. In general, a constant (bandwidth)·(voltage-gain) product was obtained as expected. With the circuit adjusted to give maximum gain of 18 db at $f_s=(f_{p/2})-10$ mc, a bandwidth of 8 mc was measured to the 3-db down points.

The most important measurement to be reported for the negative resistance amplifier is its noise figure. Because of the nature of the amplification process, noise appears in frequency band f_s at the output due to: 1) input noise at f_s which is amplified, 2) input noise at f_{p-s} which is converted to f_s in the amplification process, 3) noise which originates in the diode at f_s and is amplified, and 4) noise from the diode at f_{p+s} which is converted to f_{p-s} in the amplification process. Because of this generation of "image" frequencies during amplification, the noise performance of this type of amplifier should be better for use with a double-sideband signal centered at $f_{p/2}$ (*i.e.*, with coherent signal frequencies at both f_s and f_{p-s}) than with a signal having the same total power but with no special symmetry about $f_{p/2}$. Amplifier noise figures as low as 3 db for this special kind of double-sideband operation have been obtained, corresponding to a 6-db noise figure for ordinary operation. However, note that (because of noise source 2) above) when the equivalent temperature of the input load is decreased, even with ordinary operation the added noise becomes less than that of an ordinary amplifier having a 6-db noise figure.

The most important source of noise in the diode is that originating as thermal noise in the series resistance, R_s. Analysis shows that the product $q_s = f_s R_s C_0$ should be minimized for best noise performance, and reasonable correlation between amplifier noise figure and q_s was obtained indeed for some ten diodes tested in the negative resistance amplifier. It will be noted that considerably lower noise figures have been obtained in the 400-mc up-modulator than in the 6-kmc amplifiers, so that these data provide further evidence for the importance of reducing q_s. They also show that in the up-modulator case the noise originating at f_{p+s} (where q_{p+s} is much larger than q_s) is not very important in comparison with f_s noise, which is amplified in the up-conversion process.

These preliminary experiments have shown the feasibility and to some extent the practicability of low-noise amplification using variable capacitance diodes. There is little doubt that better circuits will be developed which will make use of improved diodes to produce amplification with noise figures significantly lower than those reported here.

G. F. Herrmann
M. Uenohara
A. Uhlir, Jr.
Bell Telephone Labs.
Murray Hill, N. J.

A Low-Noise Wide-Band Reactance Amplifier*

The object of this letter is to summarize the results of a study of a reactance amplifier operated in the sum-frequency mode. We define a reactance amplifier generically as one in which a periodically varying reactance—obtained here by driving a nonlinear capacitor with a local oscillator—is used to provide amplification of a relatively weak signal. Amplifiers (and also modulators, demodulators, oscillators, harmonic and subharmonic generators, and bistable stages) of this generic type have a long history.[1] Current interest in such amplifiers is based principally on the expectation that low-noise amplification should be obtainable if a nearly ideal reactance is used for the essential element.[2] Our results indicate that very low effective input noise temperatures are indeed realizable.[3]

In the sum-frequency mode of operation, the reactance amplifier constitutes an amplifying modulator in which the output is derived from a circuit resonant to the sum of the local oscillator frequency and the (usually much lower) signal frequency. The amplified output signal is subsequently demodulated in a receiver whose input is tuned to the sum frequency. This form of reactance amplifier also has been described as a noninverting modulator,[4] as an up-converter,[5] and as a noninverting conversion transducer.[6] The maximum available power gain of the amplifier, obtained with a lossless input circuit, is equal to the ratio of sum frequency to signal frequency. Thus appreciable gain is possible; this is important because the minimum achievable over-all effective input noise temperature is set by the post-receiver effective input noise temperature divided by the available gain. The amplifier is inherently stable because the real part of its input and output admittances is positive. Furthermore, its frequency response is formally identical with that of two tuned circuits coupled by a capacitance, so that the overcoupled condition can be utilized if desired. For these reasons, high gain and wide bandwidth are compatible, in contrast with the performance of the negative conductance forms of reactance amplifier designated as parametric amplifiers.[7–9]

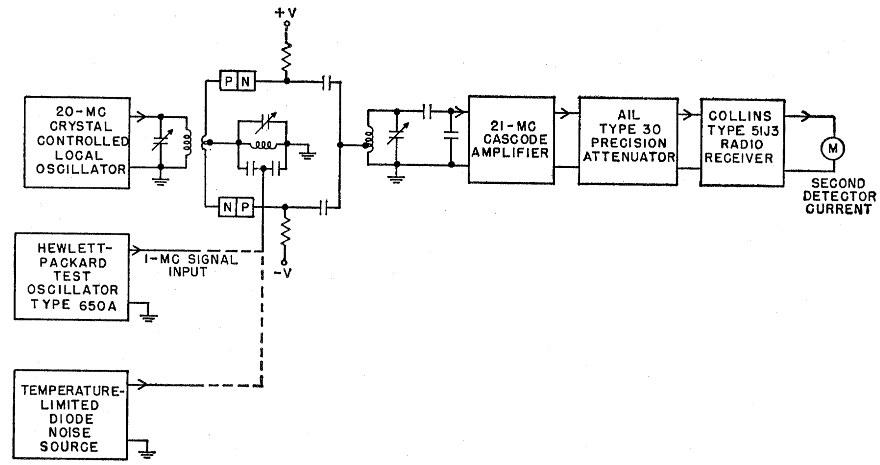

Fig. 1—Setup for measurement of balanced reactance amplifier characteristics.

To ascertain how closely theoretical performance could be achieved, a low-frequency amplifier was set up. The balanced arrangement that was used, shown schematically in Fig. 1, is a low-frequency version of the conventional balanced microwave mixer. It has the desirable features of ease of tuning, cancellation of local oscillator noise, and elimination of local oscillator current through the input and output circuits. The essential nonlinear reactance element is provided by the transition capacitance of a reverse-biased junction diode.[10] Two approximately identical commercially available (Hoffman 1N470) silicon diodes were used in the balanced arrangement. At the low operating frequencies for which the amplifier was designed, these diodes provide a nonlinear capacitance that is nearly ideal with respect to Q and to low reverse current, even at room temperature. The amplifier was supplied by a 600-ohm signal generator and coupled by an output circuit to the essentially open-circuit input terminals of a cascode amplifier. The design was approximately optimized to achieve a minimum over-all effective input noise temperature.

The main performance characteristics are listed in Table I.

TABLE I

Signal frequency	1 mc
Local oscillator frequency	20 mc
Output frequency	21 mc
Bandwidth, referred to signal frequency	10 per cent
Available power gain*	10 db
Amplifier effective input noise temperature*	30°K
Over-all effective input noise temperature	40°K

* These values include the degradation of the output circuit, which was included in the measurement for convenience.

The effective input noise temperatures in Table I were obtained with diodes and circuits operating at room temperature. Supplementary measurements made with the input circuit immersed in liquid nitrogen indicate that thermal noise originating in that circuit is a large part of the residual noise.

Extension of this study to higher frequencies is in progress. It is planned to submit a fuller account of our work at a later date.

We wish to thank A. Barone for helping us with the experimental work.

B. Salzberg
E. W. Sard
Airborne Instruments Lab., Inc.
Mineola, N. Y.

* Received by the IRE, April 4, 1958.

[1] A useful general reference is *Proc. Symp. Nonlinear Circuit Analysis, April 25–27, 1956*, Polytechnic Institute of Brooklyn, Brooklyn, N. Y.; 1957. Many of the papers included in this reference have extensive bibliographies.

[2] A. van der Ziel, "On the mixing properties of non-linear condensers," *J. Appl. Phys.*, vol. 19, pp. 999–1006; November, 1948.

[3] A recently proposed IRE Standard defines effective input noise temperature as $T_e = (F-1)T_0$, where F = noise factor and $T_0 = 290°K$.

[4] J. M. Manley and H. E. Rowe, "Some general properties of nonlinear elements—Part I. General energy relations," Proc. IRE, vol. 44, pp. 904–913; July, 1956.

[5] A. Uhlir, Jr., "Two-terminal *p-n* junction devices for frequency conversion and computation," Proc. IRE, vol. 44, pp. 1183–1191; September, 1956.

[6] C. F. Edwards, "Frequency conversion by means of a nonlinear admittance," *Bell Sys. Tech. J.*, vol. 35, pp. 1403–1416; November, 1956.

[7] H. Heffner and G. Wade, "Noise, Gain and Bandwidth Characteristics of the Variable Parameter Amplifier," presented at the Electron Devices Meeting, Washington, D. C.; November 1, 1957.

[8] S. Bloom and K. K. N. Chang, "Theory of parametric amplification using nonlinear reactances," *RCA Rev.*, vol. 18, pp. 578–593; December, 1957.

[9] T. J. Bridges, "A parametric electron beam amplifier," Proc. IRE, vol. 46, pp. 494–495; February, 1958.

[10] L. J. Giacoletto and J. O'Connell, "A variable-capacitance germanium junction diode for uhf," *RCA Rev.*, vol. 17, pp. 68–85; March, 1956.

Measurement of the Correlation Between Flicker Noise Sources in Transistors*

The flicker noise sources in a transistor can be represented by a noise emf e_e in series with the emitter junction and a noise current generator i in parallel with the collector junction. (See Fig. 1.) According to Fonger's theory[1] of flicker noise in transistors these two quantities should be strongly correlated. It is the aim of this note to present measurements of this correlation.

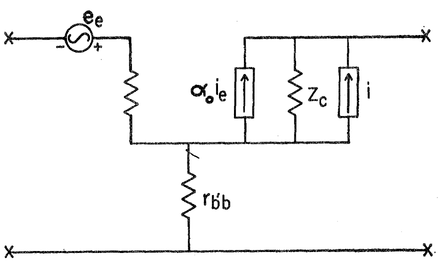

Fig. 1—Flicker noise generators in a junction transistor.

In order to present[2] the measurements in terms of the quantities e_e and i, we put $e_e = e_e' + e_e''$, where e_e' represents the part of e_e that is fully correlated with i and e'' the part of e_e that is uncorrelated with i. If the total flicker noise is now represented by an equivalent emf e_{if} in series with the emitter, we have:

$$e_{if} = e_e'' + \frac{i}{\alpha_o}\left[R_s + R_{eo} + r_{b'b} + \frac{\alpha_o e_e'}{i}\right]. \quad (1)$$

Introducing the flicker noise resistance R_{nf} by equating:

$$\overline{e_{if}^2} = 4kTR_{nf}\Delta f, \quad (1a)$$

one obtains

$$R_{nf} = R_{fl} + g_{fl}(R_s + R_{eo} + r_{b'b} + R_{fc})^2 \quad (2)$$

where R_s is the source impedance, and

$$\overline{e_{fl}''^2} = 4kTR_{fl}\Delta f; \quad \overline{i^2}/\alpha_o^2 = 4kTg_{fl}\Delta f;$$

$$R_{fc} = \frac{\alpha_o e_e'}{i} = \frac{\alpha_o \overline{e_e i}}{\overline{i^2}}. \quad (2a)$$

Here R_{fl} is the uncorrelated emitter noise resistance, g_{fl} the flicker noise conductance and R_{fc} the correlation resistance. Hence, if $\sqrt{R_{nf} - R_{fl}}$ is plotted as a function of the source impedance R_s, one should obtain a straight line:

$$\sqrt{R_{nf} - R_{fl}} = \sqrt{g_{fl}}(R_s + R_{eo} + r_{b'b} + R_{fc}). \quad (3)$$

The straight line intercepts the zero axis at:

$$R_s = R_{so} = -(R_{eo} + r_{b'b} + R_{fc}). \quad (4)$$

In the case where e_e and i are fully correlated, one has $R_{fl} = 0$ and hence

$$\sqrt{R_{nf}} = \sqrt{g_{fl}}(R_s + R_{eo} + r_{b'b} + R_{fc}). \quad (3a)$$

* Received by the IRE, March 24, 1958. This work was supported by U. S. Signal Corps Contract.

[1] W. H. Fonger, "A determination of 1/f noise sources in semiconductor diodes and transistors," in "Transistors I," RCA Labs., Princeton, N. J., pp. 239–297; 1956.

[2] A. van der Ziel, "Noise in junction transistors," this issue, p. 1019.

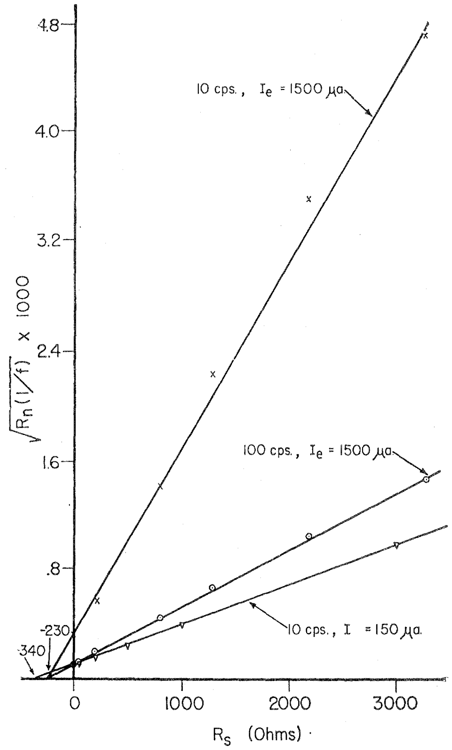

Fig. 2—$\sqrt{R_{nf}}$ vs R_s or a 2N105 transistor

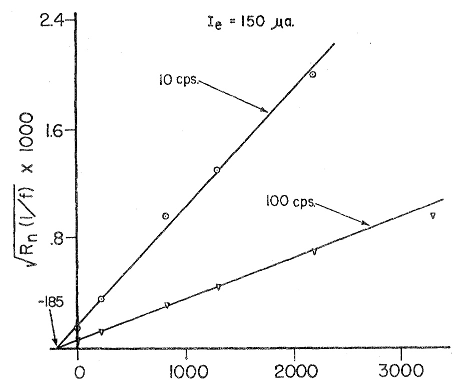

Fig. 3—$\sqrt{R_{nf}}$ vs R_s for a silicon *p-n-p* transistor.

Measurements of $R_{nf}R_s$ have been made for several transistors. Each experimental value of R_{nf} was obtained by measuring the noise spectrum of the transistor with R_s as a parameter and then subtracting the frequency-independent portion of the noise resistance from the total noise resistance at the frequency of interest.

The results of measurements on a 2N105 *p-n-p* germanium transistor are shown on Fig. 2; the results of measurements on a silicon *p-n-p* transistor are shown on Fig. 3. The fact that these curves are linear indicates that R_{fl} is practically zero, so that the noise generators are completely correlated. The slope of the curves increases with decreasing frequency and with increasing current; this is as expected for flicker noise.

Looking at Fig. 2, both the 10 cps, 1500 μa and 100 cps, 1500 μa curves intercept the R_s axis at $R_s = -230$ ohms. When I_e was decreased to 150 μa the intercept moved to -340 ohms. Direct measurement of $r_{b'b}$ for this transistor gave $r_{b'b} = 180$ ohms. The difference between this value and the intercept is attributed to the term $(R_{eo} + R_{fc})$ in (4).

The curves of Fig. 3, measured at $I_e = 150$ μa, show $R_{so} = -185$ ohms. This is also the value obtained for $r_{b'b}$ by direct measurement.

The current dependence of R_{eo} is well known ($R_{eo} \approx 26/I_e$, where I_e is the dc emitter current in ma). The current behavior of R_{fc} is not as well established; the results expected from Fonger's theory are given by van der Ziel.[2]

The measurements indicate that the quantities e_e and i are fully correlated within the limit of accuracy of the measurement.

The author is grateful to Dr. A. van der Ziel for suggesting this experiment and for much helpful advice.

EUGENE R. CHENETTE
Electrical Engineering Dept.
University of Minnesota
Minneapolis, Minn.

On the Effect of Base Resistance and Collector-to-Base Overlap on the Saturation Voltages of Power Transistors*

A recent note[1] presented a method of measuring collector and emitter resistances. This method is an excellent one for transistors having primarily extrinsic base resistance. It is the purpose of this letter to show the differences which are observed on transistors having a relatively large intrinsic base resistance, or having an extended collector to base overlap diode shunting the base resistance to the collector.

The case discussed here is recognized by the fact that the collector voltage, in the saturation region, is clamped to a value just below the base driving voltage in a grounded emitter circuit.[2] Fig. 1 shows the simplified lumped equivalent circuit assumed here. Emitter and base resistances are those normally determined from the geometry of the transistor. We neglect any additional extrinsic base resistance, as its effect is readily added to the base voltage in a more detailed analysis. We assume an ideal transistor with (external) body resistances R_E, R_B, and R_C shunted at the base contact by a base-to-collector diode D with body resistance R_D. The actual case of distributed resistances, particularly in diffused layer transistors or bonded contacts, differs only slightly from the results obtained from the lumped model.

In the practical cases where the base resistance, due to spreading effects or the large

* Received by the IRE, March 4, 1958. This work was supported by the Industrial Mobilization Div., U. S. Signal Corps, Contract No. DA-36-039-SC-72714.

[1] B. Kulke and S. L. Miller, "Accurate measurement of emitter and collector resistances in transistors," PROC. IRE, vol. 45, p. 90, January, 1957.

[2] H. G. Rudenberg and G. Franzen, "An alloy type medium power silicon transistor," 1957 IRE NATIONAL CONVENTION RECORD, pt. 3, pp. 26–31.

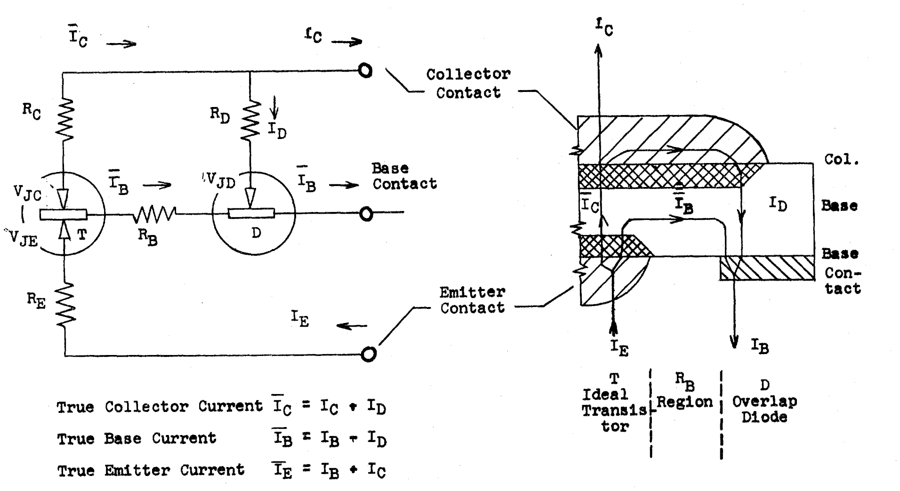

Fig. 1—Equivalent circuit

contact spacing, is relatively large, the collector voltage can only drop to a value just below the (intrinsic) base voltage referred to the emitter. Then the contact overlap diode D conducts and clamps the collector voltage, so that part of the base input current is directed to the collector contact.

We therefore obtain

$$
\begin{aligned}
V_{BE} &= R_E I_E + V_{JE} + R_B \bar{I}_B \\
&= R_E(I_B + I_C) + V_{JE} + R_B(I_B - I_D). \qquad (1)
\end{aligned}
$$

Substituting the nominal current gain of the ideal transistor $\beta = \bar{I}_C/\bar{I}_B$ we obtain the relations

$$
\begin{aligned}
\bar{I}_B &= \frac{I_B + I_C}{\beta + 1} \\
\bar{I}_C &= \frac{\beta}{\beta + 1}(I_B + I_C) \\
I_D &= \frac{\beta I_B - I_C}{\beta + 1}, \qquad (2)
\end{aligned}
$$

thus leading to

$$
V_{BE} = V_{JE} + \left(R_E + \frac{R_B}{\beta + 1}\right)(I_B + I_C), \qquad (3)
$$

and as V_{JE} is primarily a function of the emitter current $(I_B + I_C)$, we may readily test this result for various combinations of I_B and I_C. Fig. 2 illustrates this result on an alloy transistor having negligible emitter and collector resistances. Eq. (3) contrasts with the case of a transistor without overlap diode. $(R_D = \infty.)$

$$
V_{BE} = V_{JE} + R_E(I_B + I_C) + R_B I_B. \qquad (4)
$$

It is readily realized that both equations agree at full collector current $I_C = \beta I_B$ but differ at $I_C < \beta I_B$ down to $I_C = 0$ where (3) gives a much lower base voltage, which is actually observed.

Now the collector voltage may be derived from either current path

$$
\begin{aligned}
V_{CE} &= V_{BE} - V_{JD} - R_D I_D \\
&= V_{BE} - V_{JD} - R_D \frac{\beta I_B - I_C}{\beta + 1}. \qquad (5)
\end{aligned}
$$

At the knee of the saturation curve, the current through D is neglible, for $I_C \cong \beta I_B$ and the last term drops out (provided $R_D \cong R_C$). This leads directly to $V_{CE} = V_{BE} - V_{JD}$, and

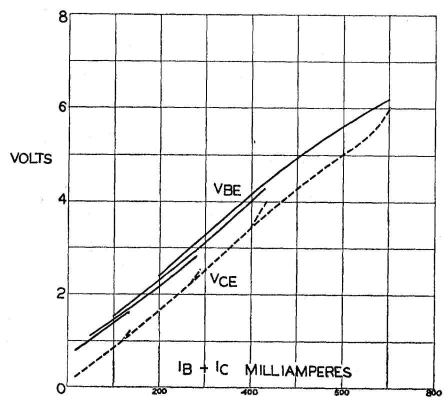

Fig. 2—Saturation voltage.

at low forward currents $(I_D = 0)$ V_{JD} is of the order of 0.2–0.3 volt (germanium) or 0.5–0.7 volt (silicon).

Interpretations of measurements taken at zero collector current differ considerably from the results of Miller. The base resistance and overlap diode lead to current circulating through the transistor even though the external current I_C is zero. Here we have at $I_C = 0$

$$
\begin{aligned}
V_{CE} &= (V_{JE} - V_{JC}) + R_E I_B + R_C \bar{I}_C \\
&= (V_{JE} - V_{JC}) + R_E I_B + R_C I_B \frac{\beta}{\beta + 1} \qquad (6)
\end{aligned}
$$

so that the resulting resistance is here

$$
R_E + \frac{\beta}{\beta + 1} R_C
$$

and not just R_E as in Miller's case.

Alternately we may solve from (5) to obtain

$$
\begin{aligned}
V_{CE} = (V_{JE} - V_{JD}) &+ \left(R_E + \frac{R_B}{+1}\right) I_B \\
&- R_D I_B \frac{\beta}{\beta + 1}. \qquad (7)
\end{aligned}
$$

Here the effective resistance, after subtracting the other junction voltages, is given by

$$
R_E + \frac{R_B}{\beta + 1} - \frac{\beta R_D}{\beta + 1}. \qquad (8)
$$

The choice between (6) and (8) is slight as (5) and (7) are equal and are two equations for solving the network currents.

For cases of negligible R_D there remains an added resistance $R_B/\beta + 1$ obtained from the same experimental conditions which, in the absence of such base resistance, gives only R_E. In the example of Fig. 2 the base resistance can be directly measured between two opposite base tabs, and leads to $R_b = 50$ ohms for both tabs in parallel. It is known that R_E is less than 0.1 ohm for this unit, so that the measured collector saturation resistance of 8.3 ohms is entirely due to the base resistance overlap to the collector.

Similar effects are noted in cases where R_C or R_D are large compared to R_B/β, and these cases can be calculated from analogous derivation. In all the cases where the collector is only driven into apparent saturation by being clamped to the base voltage, the storage time is correspondingly reduced to the pulse recovery time of the base-to-collector diode. The overlap diode here takes the place of an external diode in preventing operation in the (true)[3] saturation region of the transistor.

H. Gunther Rudenberg
Transitron Electronic Corp.
Wakefield, Mass.

J. J. Ebers and J. L. Moll, "Large signal behavior of junction transistors," Proc. IRE, vol. 42 pp. 1761–1772; December 1956.

Voltage Feedback and Thermal Resistance in Junction Transistors*

It is well known that the static characteristics of a transistor only can be used to give an approximate value of the transistor small signal parameters provided the effects of heating, which invariably occur to some extent, are kept to negligible proportions. However, it is not always appreciated that the voltage-feedback characteristic is dominated by thermal effects at all normal operating currents of a transistor, and only at collector currents of several microamps in low-level transistors or a few milliamps in power transistors can these effects be ignored. It is the purpose of this note to point out that this effect of transistor heating can be used conveniently to measure a transistor's thermal resistance.

For the measurement of thermal resistance it is necessary to consider the transistor in the common-base configuration so that emitter current can be held constant. Two kinds of feedback may be distinguished whose sum represents the total observed feedback. Firstly, there is the usual electrical feedback resulting from collector space-charge layer widening and extrinsic base resistance as described by Early.[1]

* Received by the IRE, December 30, 1957; revised manuscript received, March 27, 1958.

[1] J. M. Early, "Effect of space charge layer widening in junction transistors," Proc. IRE, vol. 40, pp. 1401–1406; November, 1952.

Thus,

$$h_{rb}\ (\text{electrical}) = \left.\frac{\partial V_{eb}}{\partial V_{cb}}\right|_{I_e, T_e} \qquad (1)$$

where T_e is the emitter junction temperature.

Using Early's notation and results,

$$h_{rb}\ (\text{electrical}) = (r_b' + r_b'')g_c' \qquad (2)$$

and if emitter efficiency is unity,

$$r_b'' = r_e'/2(1 - \alpha'). \qquad (3)$$

To a first approximation r_b', the extrinsic base resistance, and α' the common-base current gain are independent of I_e, while the emitter conductance $1/r_e'$, and g_c', the collector conductance, are proportional to it. The variation of h_{rb}(electrical) with I_e is consequently as shown in Fig. 1, curve (a).

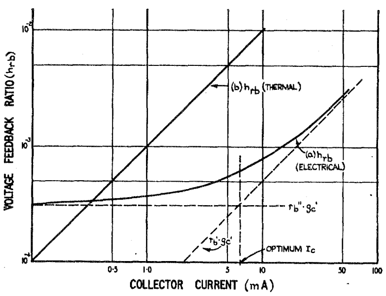

Fig. 1—The dependence of voltage feedback ratio upon emitter current.

It will be explained later that the optimum current for thermal resistance measurement is at the point where h_{rb}(electrical) changes from being constant to being proportional to I_e, that is, where $r_b' = r_b''$.

Secondly there is the thermal feedback. In computing its value the electrical feedback will temporarily be ignored.

Thus,

$$h_{rb}\ (\text{thermal}) = \left.\frac{\partial V_{eb}}{\partial V_{cb}}\right|_{I_e}$$

$$= \left.\frac{\partial V_{eb}}{\partial T_e}\cdot\frac{\partial T_e}{\partial P}\cdot\frac{\partial P}{\partial V_{cb}}\right|_{I_e} \qquad (4)$$

where P is the total power dissipated in the transistor. Now, since $I_e \propto I_{eo} \exp(qV_{eb}/kT)$ and I_{eo} increases by about 10 per cent per degree centigrade, it follows that when I_e is constant in germanium transistors

$$\left.\frac{\partial V_{eb}}{\partial T_e}\right|_{I_e} \approx 0.0025 \text{ volts/°C}. \qquad (5)$$

If it is assumed that in thermal equilibrium the emitter junction is at the same temperature as the collector junction, then $\partial T_e/\partial P = \theta$, the thermal resistance of the transistor.

Assuming that all the heat is dissipated at the collector junction,

$$\left.\frac{\partial P}{\partial V_{cb}}\right|_{I_e} = I_c + V_{cb}\frac{\partial I_c}{\partial V_{cb}} \approx I_c. \qquad (6)$$

(The signs of the right-hand sides of (5) and (6) refer to n-p-n transistors. For p-n-p transistors they are both negative.)

Eq. (4) can now be written

$$h_{rb}\ (\text{thermal}) = 0.0025 \cdot \theta \cdot I_c. \qquad (7)$$

The variation of h_{rb} (thermal) is shown in Fig. 1, curve (b).

Since h_{rb} (total) $= h_{rb}$ (thermal) $+ h_{rb}$ (electrical) and since for the measurement of θ only the thermal feedback is required, it is desirable to reduce the electrical feedback as far as possible. Above the optimum current previously referred to the electrical feedback remains a constant and minimum fraction of the total feedback-voltage ratio, so that measurements of h_{rb} should be made within this region. However, since it is the change in V_{eb} that is measured, it is desirable to change V_{cb} (and hence V_{eb}) by as much as possible; I_c therefore should be kept as low as possible so that at the maximum value of V_{cb}, the transistor rated power dissipation, is not exceeded. The value of I_e at which $r_b' = r_b''$ often roughly optimises these conflicting requirements.

The time constants of the two kinds of voltage feedback are very different. The electrical feedback remains constant up to at least a few hundred cycles in most transistors, but the thermal feedback only assumes the value given in (7) after sufficient time has elapsed for thermal equilibrium to be reached, which may be a matter of minutes. It is clear therefore that to determine θ from h_{rb} it is necessary to use a dc method of measurement. (Typically thermal feedback contributes about 10 per cent of the modulus of the total feedback at 10 cycles per second, whilst at dc it may contribute 95 per cent).

The curves given in Fig. 1 are typical of a low-level transistor measured at dc. They refer to a transistor in which $r_b' = 100$ ohms, $\alpha' = 0.98$, $g_c' = 0.5$ μmho when $I_c = 1$ma and $\theta = 0.4$°C/mw. The relative importance of thermal feedback can readily be seen.

The effect also, of course, appears in the common emitter configuration, but here the thermal feedback ratio is negative although the electrical feedback remains positive. The characteristics shown in Fig. 2, which are

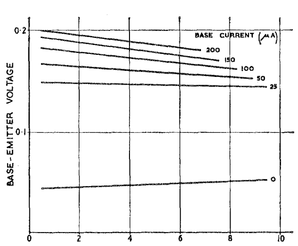

Fig. 2—Common-emitter voltage feedback characteristics.

taken directly from published data, show clearly a negative slope except at the lowest current level. Evidently, therefore, these curves simply record the heat generated by varying the collector voltage and may be misinterpreted if this fact is not appreciated.

J. J. Sparkes
British Telecommun. Res.
Taplow Court,
Taplow, Bucks., England

Microwave Transients from Avalanching Silicon Diodes*

During a study of diffused p-n junction silicon diodes, it was noticed that in a certain range of breakdown current appreciable energy was being radiated in the 9 kmc region. The particular diodes under study were fabricated in a way which results in a maximum impurity gradient in the center of the diode, with the gradient falling off rapidly away from the center. This situation is favorable for breakdown occurring in a single point, with a resulting single microplasm. This was confirmed by observation of a single set of pulses which disappear and are replaced by steady conduction as current is increased.[1]

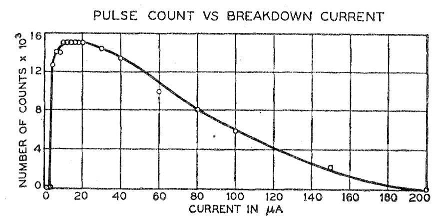

Fig. 1—Pulse count vs average current. The qualitative shape of this curve shows that the breakdown occurs in a single microplasma.

Fig. 1 shows pulse count vs current, with steady conduction setting in at 150 μa.

It was desired to relate in time the occurrence of the pulses and radiation of 9-kmc energy. For this purpose, the circuit of Fig. 2 was arranged and photographs of single simultaneous traces on each oscilloscope were taken. The 545 oscilloscope recorded the occurrence and duration of the current pulses and the 517A recorded the output of the 9-kmc receiver.

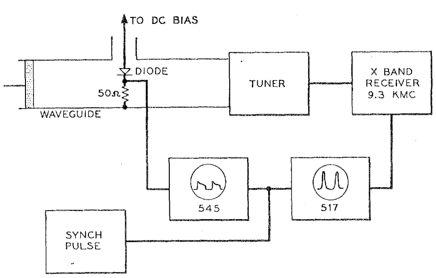

Fig. 2—Block diagram of circuit used for measurements of current and receiver output. The synchronizing pulse was arranged to give single oscilloscope traces which were photographed. The different trigger delay of the two oscilloscopes was accounted for by placing the same signal on the vertical axes and comparing the resulting traces.

Fig. 3 is a composite tracing taken from the oscillograph picture. The traces are rearranged in this way to allow the use of the same time axis in each case. The simultaneity of the turn-on of the current pulse and the radiation of energy is beyond doubt.

The width of the output pulses from the receiver is about ½ μsec in agreement with the receiver bandwidth of about 1 mc. It is interesting to note that the turn-off does not

* Received by the IRE, March 21, 1958.

[1] K. G. McKay, "Avalanche Breakdown in Silicon," *Phys. Rev.*, vol. 94, p. 877; May, 1954.

produce a radiation, indicating that it is much slower than the turn-on of the pulses. This is an expected result since the turn-off time is controlled by passive circuit parameters while the turn-on is controlled by the low dynamic impedance of the microplasma.

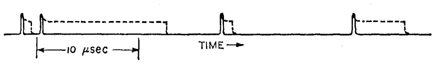

Fig. 3—Simultaneous oscillograph tracings of diode current and output of microwave receiver. The dotted curve is the current and shows a slight initial overshoot. The overshoot as well as the observed rise and fall times are characteristic of the measuring circuit. The solid curve is the 9-kmc receiver output. In every case the pulse rise results in a pip from the receiver.

By comparison with an argon lamp noise source, it was determined (for another one of the diodes) that the average power at 9 kmc was 32 db above thermal noise when the pulse rate N was 5×10^6 per second. If the leading edge of the pulse is a step Δi in current, the energy per pulse is

$$\frac{B(\Delta i)^2R}{2\pi^2f^2},$$

where R is the effective impedance shunting the step, and B is bandwidth. The ratio to thermal noise is therefore

$$\frac{(\Delta i)^2RN}{2\pi^2f^2kT}.$$

The pulse height for this diode was 400 μa. For an effective shunting resistance of 10^4 to 10^5 ohms (the estimated value for the tuning that was used), the calculated ratio of average power to thermal power is in the range of 20 to 30 db in good agreement with the measured value.

Thus it is a reasonable conclusion that the radiated energy is the Fourier component in the 9-kmc region. This conclusion requires that the current step occur in the order of 10^{-11} or less seconds, which is in agreement with previous calculations.

The authors wish to acknowledge the help of Dr. N. G. Cranna, who directed the fabrication of the diodes.

J. L. Moll
A. Uhlir, Jr.
B. Senitzky
Bell Telephone Labs.
Murray Hill, N. J.

A Harmonic Generator by Use of the Nonlinear Capacitance of Germanium Diode*

Until recently, silicon diodes have been used for the millimeter wave harmonic generator. The writer used the gold-bonded germanium diode as the harmonic generator of 48 Gc[1] from 24 Gc and fairly good results were obtained.

The harmonic generator used in our experiment is of so-called "open guide" type; that is to say, where a germanium crystal and a gallium doped gold whisker are in direct contact in a 48 Gc waveguide. After the whisker is contacted to the crystal, a forming voltage is applied to make a gold-bonded contact. Then a suitable external negative bias voltage must be supplied to the diode in order to obtain the maximum harmonic power. An output of 1.4 mw at 48 Gc is obtained as the maximum output power at the 80-mw input of 24 Gc and the best efficiency obtained is -15.8 db at 10-mw input power. A typical variation of 48 Gc output power and diode current vs supplied negative bias voltage is show in Fig. 1. A remarkable fact is that the maximum output power is obtained in the region where negative diode current flows. Fig. 2 shows the voltage-current characteristic of the diode which is used in this experiment.

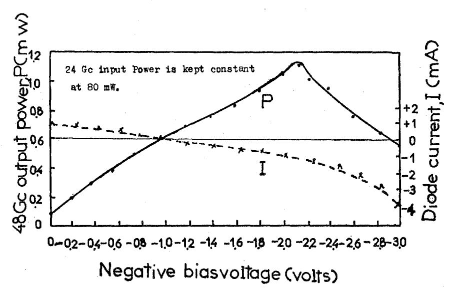

Fig. 1—48 Gc output power and diode current vs supplied negative bias voltage.

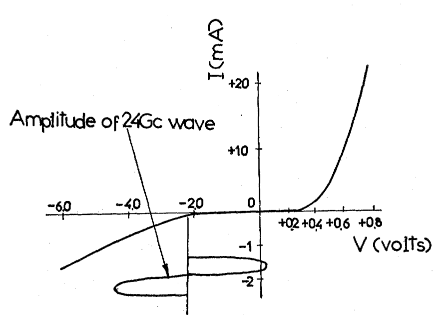

Fig. 2—Voltage-current characteristic of the diode.

This suggests that the most part of the amplitude of 24 Gc wave operates in the reverse region of the diode as shown in Fig. 2. It is believed, therefore, that the harmonic generation is caused by the nonlinearity of diode's barrier capacitance, because the nonlinearity of the reverse resistance is much smaller than that of the forward resistance.

The diode impedance in 24 Gc was measured, and it was found that in the forward bias region of 0 to 0.6 volt only the resistance component varied and in the reverse bias region of 0 to -2.0 volts the resistance component remained constant, while the reactance component varied appreciably. These results might support the above-mentioned reasoning that the harmonic generation is due mainly to the nonlinear barrier capacitance of the germanium diode.

Another merit of this harmonic generator is its large power-handling capacity. This diode could withstand the input power of the order of 300 mw without causing any noticeable change in the diode character. Millimeter wave of several milliwatts in power will be obtained if sufficiently higher input power is available.

I wish to thank Y. Nakamura, Dr. B. Oguchi, and M. Watanabe of the Electrical Communication Laboratory for helpful discussions and suggestions.

Shoichi Kita
Electrical Communication Lab.
Nippon Telegraph and
Telephone Public Corp.
Tokyo, Japan

* Received by the IRE, February 3, 1958.
[1] 1 Gc $=10^9$ cycles.

On Junctions Between Semiconductors Having Different Energy Gaps*

Recently there has been some interest in the properties of junctions between two semiconductors having different energy gaps,[1] such as silicon-germanium alloy of two different compositions. In general, the concentration of holes and electrons will be different on each side of the junction.

Of course, this is also true of a junction between two regions of the same semiconductor, but with different doping densities. In that case, however, there is the condition that the product of hole and electron density be the same on each side of the junction, at equilibrium. This result can be considered as arising from the compensating effects of current due to diffusion and due to the field at the junction; the electron current J_n, for instance, is given by

$$J_n = D_n\left\{\frac{dn}{dx} + \frac{q}{kT}E(x)n\right\} \tag{1}$$

and a similar equation for J_p. D_n is the diffusion constant, n the electron density, coulombs per unit volume, q the electronic charge, $E(x)$ the field, T the temperature. If $J_n = J_p = 0$, by eliminating $E(x)$ from the two resulting equations, one obtains pn = constant. Thus, the junction can be described in terms of the hole and electron densities on each side, and the junction field; and the width of the energy gap, which is taken as fundamental in some treatments, here has disappeared, merely determining, or being a statement of, the electron and hole concentrations on each side of the junction.

When the junction is between two different semiconductors, one can write

$$\left.\begin{aligned} J_n &= D_n\left\{\frac{dn}{dx} + \frac{q}{kT}E_n(x)n\right\} \\ J_p &= D_p\left\{-\frac{dp}{dx} + \frac{q}{kT}E_p(x)p\right\} \end{aligned}\right\}. \tag{2}$$

E_n and E_p are the fields as "seen by" electrons and holes, respectively, and are not

* Received by the IRE, January 13, 1958.
[1] H. Kroemer, "Quasi-electric and quasi-magnetic fields in nonuniform semiconductors," *RCA Rev.*, vol. 18, pp. 332–342; September, 1957.

necessarily the same. In fact, if $J_n = J_p = 0$, one can obtain

$$\left.\begin{aligned}\int \{E_p(x) - E_n(x)\} dx &= C_- + \frac{kT}{q} \ln (pn) \\ \int \{E_p(x) + E_n(x)\} dx &= C_+ + \frac{kT}{q} \ln \left(\frac{p}{n}\right)\end{aligned}\right\} \cdot (3)$$

C_- and C_+ are constants. It is apparent that if pn is different in different places, E_p and E_n will be different. In fact, the variation in pn implies a variation in the width of the energy gap, and E_p and E_n can be interpreted in terms of the slope of the lower and upper edges of the forbidden band, respectively.

These influences which are different for charges of one sign than for those of the other have been called "quasi-electric" fields.[1] They may appear at first sight to be something of a very strange or "quantum" nature. It may be worthwhile, accordingly, to point out that something like this may be seen to arise from quite simple and elementary considerations.

Suppose that the two kinds of semiconductor have different dielectric constants; in general, this will be true. Then a charge $\pm q$, near the junction, will experience an image force F, given by[2]

$$F = \frac{1}{4\pi\epsilon_1}\left(\frac{\epsilon_1 - \epsilon_2}{\epsilon_1 + \epsilon_2}\right)\frac{q}{4a^2} \qquad (4)$$

ϵ_1 and ϵ_2 being the permittivities of the two semiconductors (the charge is in semiconductor 1) and a the distance of the charge from the junction. The force is such as to drive charges of either sign into the semiconductor whose permittivity is greater. Thus, this image force could be regarded as a "quasi-electric" field, E_p and E_n being equal in magnitude and opposite in sign. Thus, effects of this sort can arise on very simple classical grounds. It is interesting to notice, in this connection, that there is often a correlation between dielectric constant and energy gap in semiconductors. Fig. 1 shows this relation for the series carbon (diamond), germanium, silicon, and grey tin. The values used are from information believed to be the most recent. It is apparent that the energy gap decreases with increasing dielectric constant, more or less as the square. This correlation is in the right direction, for one would expect carriers to concentrate in the material of higher dielectric constant, just as one expects their density to be greater in the material of smaller energy gap.

Analogous "quasi-magnetic" fields could arise similarly.[1] Consider a charge moving parallel to a junction between two semiconductors of different magnetic permeabilities. Again there would be an image force, in a direction perpendicular to the plane of the junction. The force would be in the same sense for charge of both signs, just as happens with an ordinary magnetic field; but, since the square of the velocity of the charges would enter into the relations, the "quasi-magnetic" field "seen" by various carriers would be proportional to their respective mobilities.

[2] G. P. Harnwell, "Principles of Electricity and Electromagnetism," 2nd ed., McGraw-Hill Book Co., Inc., New York, N. Y., pp. 72–74; 1949.

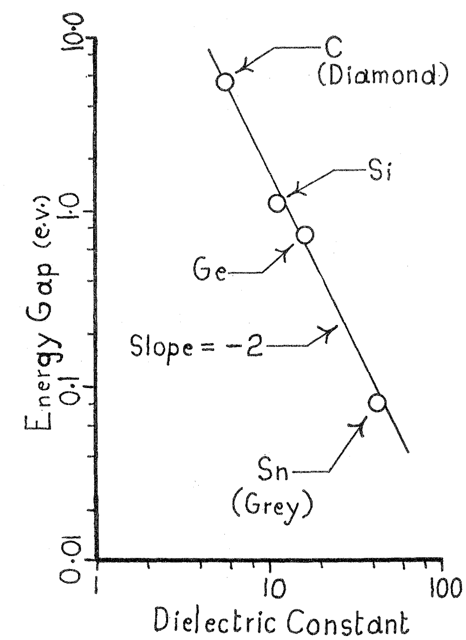

Fig. 1—Energy gap E_g vs dielectric constant for several semiconductors of similar crystal structure. There is approximately an inverse square relationship.

In conclusion, there is a point in connection with all this which it may be interesting to consider. Suppose that there is a junction between two different semiconductors. The one will have a fairly wide energy gap, and be (say) n type, for definiteness. The other semiconductor will have a quite narrow energy gap. Then, as can be seen in Fig. 2, the form of the energy zones will be about the same whether the material with the narrow energy gap is p type, n type, or intrinsic. Accordingly, it might as well be intrinsic, and junctions of this sort might have the generic name e-i_+ (extrinsic to super intrinsic). This would add another generic type of junction to the p-n junction and the L-H (low to high doping, such as n to super-n) junction.[3]

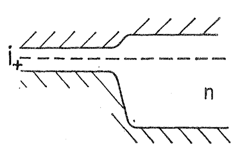

Fig. 2—Energy band scheme of a particular case of an e-i_+ (here an n-i_+) junction. The Fermi level is shown dashed, and the diagram is plotted in terms of electron energy, as is usual.

An n-i_+ junction, as shown in Fig. 2, might be expected to have some interesting properties. For instance, the hole density on the i_+ side would be greater than that on the n side. Accordingly, if the i_+ side is driven positive, it will inject holes into the n side. This should give a result similar to the forward characteristic of a p-n junction. If, on the other hand, the i_+ region is driven negative, since the i_+ region has a greater density of electrons than has the n region, the characteristic would be similar to that of an n-n_+ junction.[3]

It is interesting to think that a contact between a metal and a semiconductor might be considered as a limiting case of an e-i_+ junction, the metal being the i_+ part, in which the energy gap in the i_+ material had disappeared entirely. Ordinarily, one does not think of a metal as an intrinsic material. However, for every conduction electron above the Fermi level in the metal, there should be a vacancy below. While it is not suggested that these vacancies take part in metallic conduction to any appreciable extent, they might be able to act like holes to the extent of being injected into a contacting semiconductor. Certainly, many metal point contacts on semiconductors act in the way suggested above for e-i_+ junctions, and it may be interesting to think of the point contacts as a special case of these junctions.

Of course, there may be surface or interface effects, such as barriers, double layers of charge, etc., at any junction between two different materials. The effects considered here would be in addition to any interface effects.

Some of the work on which the discussion is based was done when the writer was at the National Research Council, Ottawa, Canada.

H. L. ARMSTRONG
Pacific Semiconductors, Inc.
Culver City, Calif.

[3] J. B. Arthur, A. F. Gibson, and J. B. Gunn, "Carrier accumulation in germanium," *Proc. Phys. Soc. B*, vol. 69, pp. 697–704; July, 1956.
——, ——, ——, "Current gain at L-H junctions in germanium," *Proc. Phys. Soc. B*, vol. 69, pp. 705–711; July, 1956.

Arc Prevention Using P-N Junction Reverse Transient*

In the November issue I found the above article[1] by Miller.

The survey of literature indicates that the method of using semiconducting devices for arc suppression has been developed by earlier investigators and actual devices have been built using this principle. In particular I would like to quote the paper by Parrish[2] of the International Rectifier Corporation, El Segundo, Calif. This paper discusses in great detail the design and theory of arc quenching devices by means of germanium or selenium diodes. It also contains references to previous work in the same field. Since Miller does not mention the above referenced work, I assume that his duplication of effort stems from the unawareness of similar earlier work.

BERTHOLD ZARWYN
Chief Physicist
Link Aviation, Inc.
Binghamton, N. Y.

* Received by the IRE, January 29, 1958.
[1] W. Miller, PROC. IRE, vol. 46, pp. 1546–1547; November, 1957.
[2] F. W. Parrish, "Arc suppression with semiconductor devices," *Elec. Mfg.*, vol. 57, pp. 127–131, 344–346; June, 1956.

Improved Keep-Alive Design for TR Tubes*

I was very interested to read the above paper by Dr. Gould.[1] At first glance, his explanation of intermittent crystal failure behind a TR switch appears basically opposed to that previously advanced;[2] his mechanism is an anode effect whereas the glow-arc transition is essentially a cathode effect. I hope, however, to show that his results are not inconsistent with our work on this subject. First it is relevant to summarize the evidence in favor of the "cathode effect" hypothesis.

1) If the keep-alive voltage is observed on a free running oscilloscope, occasional instabilities are observed which correspond to a drop to a few tens of volts. This is fairly well established[2,3] and has been observed in many laboratories. This instability is consistent with the discharge behavior in a glow-arc transition.

2) Initially, with a clean, well-baked assembly, these instabilities do not happen. Their occurrence seems to be bound up with the formation of an oxide film on the keep-alive, which typically occurs in the first 100 hours of life.[4]

3) With rhodium keep-alives, no oxide films and no instabilities of this type are observed.[2]

4) In argon alone[4] or argon plus hydrogen[5] these instabilities do not occur.

All these results are mainly applicable to the "abnormal glow" condition of keep-alive discharge. Gould's keep-alives were in the "normal glow" condition, where transitions from glow to arc are very unlikely to occur.[4] Our experiments with "normal glow" keep-alives were discontinued because of the practical success of using two keep-alives in the abnormal glow condition. Dr. Gould's ingenious solution of the main problem of the normal glow keep-alive discharge, namely localizing the discharge in the required position, would be expected to give prolonged crystal protection. There is thus no scientific disagreement between us.

I should like to ask three questions on points that were not specifically mentioned in the article. First, is the low power performance of the TR cell as a function of life adversely affected by this arrangement? Sputtered (charged) particles follow lines of force and thus should be deposited on the outside of the cone where their effect on matching and insertion loss could be great. Second, does the interaction loss change very greatly as the water vapor is cleaned up? Third, are relaxation oscillations, which usually occur at some time with normal glow discharges, present or troublesome?

D. Walsh
Engineering Lab.
Oxford University
Oxford, Eng.

* Received by the IRE, May 7, 1957.

[1] L. Gould, Proc. IRE, vol. 45, pp. 530–533; April, 1957.
[2] T. J. Bridges, P. O. Hawkins, and D. Walsh, "Keep-alive instabilities in a TR switch," Proc. IRE, vol. 44, pp. 535–538; April, 1956.
[3] J. C. French, "Electrode deterioration in transmit-receive tubes," *J. Res. Nat. Bur. Stand.*, vol. 45, pp. 310–315; October, 1950.
[4] D. Walsh, A. W. Bright, and T. J. Bridges, "Electrode deterioration in keep-alive discharges in transmit-receive switches," *Brit. J. Appl. Phys.*, vol. 7, pp. 31–35; January, 1956.
[5] D. Walsh, "The electron affinity of hydrogen in a microwave gas discharge," *J. Electronics*, vol. 1, pp. 444–448; January, 1956.

WWV Standard Frequency Transmissions*

Since October 9, 1957, the NBS radio stations WWV and WWVH have been maintained as constant as possible with respect to atomic frequency standards maintained and operated by the Boulder Laboratories, NBS. On October 9, 1957, the U.S.A. Frequency Standard was 1.4 parts in 10^9 high with respect to the frequency derived from the UT 2 second (provisional value) as determined by the U. S. Naval Observatory. The atomic frequency standards remain constant and are known to be constant to 1 part in 10^9 or better. The broadcast frequency can be further corrected with respect to the U.S.A. Frequency Standard as indicated in the table below. This correction is *not* with respect to the current value of frequency based on UT 2. A minus sign indicates that the broadcast frequency was low.

The WWV and WWVH time signals are synchronized; however, they may gradually depart from UT 2 (mean solar time corrected for polar variation and annual fluctuation in the rotation of the earth). Corrections are determined and published by the U. S. Naval Observatory.

WWV and WWVH time signals are maintained in close agreement with UT 2 by making step adjustments in time of precisely plus or minus twenty milliseconds on Wednesdays at 1900 UT when necessary; no step adjustment was made at WWV and WWVH.

WWV Frequency†

1958 March 1500 UT	Parts in 10^9
1	−2.6
2	−2.6
3	−2.7
4	−2.8
5	−2.9‡
6	−2.9
7	−2.9
8	−3.0
9	−3.0
10	−3.0
11	−3.0
12	−2.9
13	−2.9
14	−2.8
15	−2.8
16	−2.8
17	−2.9
18	−3.0
19	−3.0
20	−3.1
21	−3.1
22	−3.1
23	−3.1
24	−3.1
25	−3.1
26	−3.1
27	−2.9
28	−2.8
29	−2.7
30	−2.7
31	−2.7

† WWVH frequency is synchronized with that of WWV.
‡ Decrease in frequency of 0.5×10^{-9} at 1900 UT at WWV.

W. D. George
Radio Standards Lab.
Natl. Bur. of Standards
Boulder, Colo.

* Received by the IRE, April 16, 1958.